The endocytic penetration mechanism of iron oxide magnetic nanoparticles with positively charged cover: A morphological approach

MAGDALENA CAÑETE[1], JORGE SORIANO[1], ANGELES VILLANUEVA[1], ALEJANDRO G. ROCA[2], SABINO VEINTEMILLAS[2], CARLOS J. SERNA[2], RODOLFO MIRANDA[3] and MARIA DEL PUERTO MORALES[2]

[1]Departamento de Biología, Universidad Autónoma de Madrid C/ Darwin 2, Cantoblanco, 28049; [2]Instituto de Ciencia de Materiales de Madrid, CSIC C/, Sor Juana Inés de la Cruz 3, Cantoblanco, 28049; [3]Departamento de Física de la Materia Condensada, Universidad Autónoma de Madrid, and IMDEA Nanociencia, Madrid, Spain

Received April 23, 2010; Accepted June 3, 2010

DOI: 10.3892/ijmm_00000496

Abstract. In this study we present a morphological approach in observing the interaction of cationic magnetic nanoparticles with A-549 cells (human lung adenocarcinoma). Under our experimental conditions, nanoparticles easily penetrated cells and were observed *in vivo*, using bright light microscopy. In fixed cells, nanoparticles remained inside cells, showing quantity and distribution patterns similar to those in unfixed cells. The presence of nanoparticles did not affect cell viability or the morphologic parameters assessed. We determined the potential internalization mechanism of nanoparticles into cells using endocytosis inhibitors. The results suggest that nanoparticles used in this study penetrate A-549 cells mainly through a macropinocytosis process.

Introduction

Magnetic iron oxide nanoparticles (NPs) are a promising tool in several biomedical fields, including cancer hyperthermia treatments, drug delivery and magnetic resonance imaging (MRI) (1,2). The use of macromolecular conjugation for the controlled delivery of low molecular weight drugs can minimize their passive diffusion in tissue systems, resulting in lower toxic treatments. It is also possible to design macromolecular complexes with high affinity to membrane receptors, in order to regulate cellular recognition of these carriers, trafficking pathway and subcellular localization (3,4). The magnetic character of the particles and its ability to enhance proton relaxation of specific tissues add enhanced functionality to these nanomaterials, allowing MRI monitorization of drug delivery (5), as well as for gene therapy or gene carrier (6).

Correspondence to: Dr Magdalena Cañete, Departamento de Biología, Universidad Autónoma de Madrid/Darwin 2, Cantoblanco, 28049 Madrid, Spain
E-mail: magdalena.canete@uam.es

Key words: magnetic iron oxide nanoparticles, A-549 cells, macropinocytosis, clathrin mediated endocytosis

Penetration of NPs may occur through various endocytic processes, such as function of the size and type of cover as well as the cell type (1,7-10). Cytoplasm membrane folds inward to form the vesicle containing the particles, indicating that it could be a non-receptor or receptor-mediated process. It is necessary to know the precise mechanism of NP internalization in cells since, depending on the endocytic process, NPs have different targets in the endosomal compartment. Thus, macropinocytosis (non-receptor-mediated process) does not lead to the lysosomal compartment, avoiding a possible degradation, while the clathrin mediated endocytosis leads the vesicle to the lysosomal compartment (3,4).

Previous studies carried out in our laboratory have shown that NPs-AD with positive charge are rapidly internalized into HeLa cells by an endocytic mechanism, having little or no toxicity (11).

In this study, we evaluated the toxicity in human lung adenocarcinoma cells (A-549) of iron oxide magnetic nanoparticles with a positive surface charge. Positively charged NPs quickly penetrated this type of cell and were easily observed in light microscopy without further staining. In addition, these NPs do not cause any negative effect in cell viability or morphology. Using inhibitors of different endocytosis pathways, we identified that the possible mechanism of internalization of these surface coated magnetic nanoparticles is mainly by a macropinocytosis process.

Materials and methods

Nanoparticles: synthesis and characterization. Cationic magnetite nanoparticles (amino-dextran, AD) were synthesized in a single step by coprecipitation of iron (II) and (III) salts in a basic solution in the presence of AD (12). An iron-salt mixture of 0.33 M $FeSO_4 \cdot 7H_2O$ and 0.67 M $Fe(NO_3)_3 \cdot 9H_2O$ in 50 ml of water was slowly added to a deoxygenated 400 ml 1 M NaOH solution containing AD, in particular DEAE-dextran (4.32 g of MW=10,000 g/mol). The mixture was magnetically stirred and kept for 5 h under a nitrogen flow. Centrifugation at 9,000 rpm was carried out in order to eliminate impurities and large aggregates. Finally, a suspension was prepared by sonication, filtered through a 0.2 μm

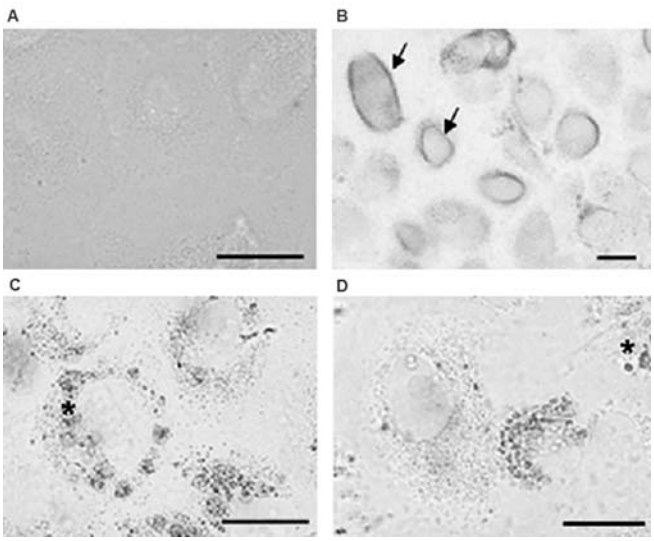

Figure 1. A-549 cells incubated with AD (0.5 mg Fe/ml) and observed *in vivo*. (A) Control cells. (B) Cells incubated with AD for 6 h and observed immediately after treatment. Arrows indicate the NP accumulation in the plasmatic membrane. Cells incubated for 24 h and observed immediately after treatment (C) and 24 h later (D). *Spot corresponds to NP accumulation. Scale bar 20 μm.

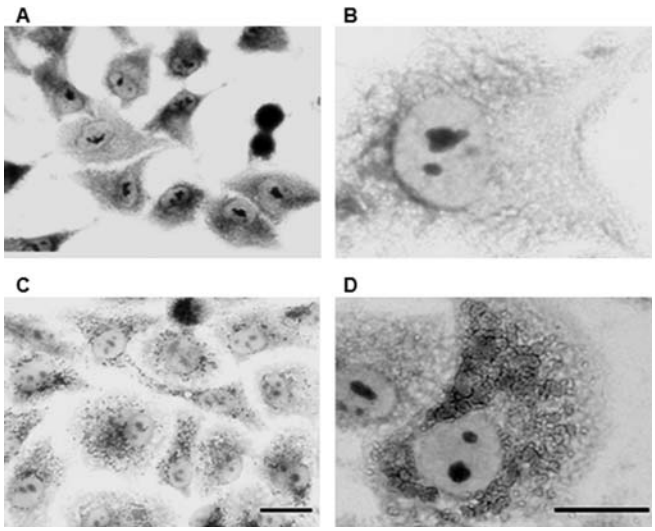

Figure 2. A-549 cells processed for TB staining. (A and B) Control cells. (C and D) Cells incubated with AD 0.5 mg Fe/ml during 24 h and processed immediately after treatment. Scale bar 20 μm.

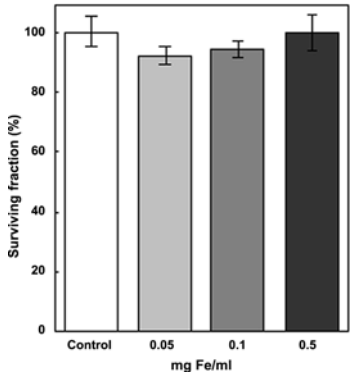

Figure 3. A-549 cell viability, measured by MTT assay 24 h after incubation with different concentrations of NPs during 24 h. Data show the average of at least three experiments ± SD.

membrane, adjusted to pH 7.0 and dialyzed to eliminate free ions (11).

Cell culture. Human lung adenocarcinoma (A-549) cells were grown in Dulbecco's modified Eagle's medium (DMEM) with 50 units/ml penicillin, 50 μg/ml streptomycin and supplemented with foetal bovine serum (FBS), at a concentration of 10%. All media, serum and antibiotics were provided by Gibco. Cell cultures were performed in a 5% CO_2 atmosphere at 37˚C and maintained in a SteriCult 200 (Hucoa-Erloss) incubator. Cells were seeded on 24-multiwell dishes with or without coverslips.

Internalization. In order to analyze the internalization of NPs, A-549 cells grown on coverslips were incubated for 1-24 h with different NP concentrations (0.05, 0.1 and 0.5 mg Fe/ml culture medium). After incubation, cells were washed three times with PBS and observed *in vivo* or processed by toluidine blue staining either immediately, at 24 h or at 48 h.

Toluidine blue staining. In order to assess the precise localization of NPs in cells after experimental procedures, cells were fixed in cold methanol (5 min) and then stained with toluidine blue (TB, 0.05 mg/ml distilled water, 0.5 min Merck), washed with distilled water and air dried. Preparations were mounted in Depex (Serva) and observed with bright field microscopy. Under these conditions, the amount and distribution of NPs remained identical to that of unprocessed cells.

Evaluation of cell viability. Viability of A-549 cells after different treatments was determined using methylthiazol tetrazolium bromide assay (MTT, Sigma). After 24 h from incubation with NPs, MTT was added to each well (100 μg/ml culture medium) for 3 h at 37˚C. The formazan formed into cells was dissolved adding 0.5 ml of DMSO in each well and the optical density was evaluated at 540 nm in a microplate reader (Tecan Spectra Fluor Spectrophotometer). Cell survival was expressed as the percentage of absorption of treated cells in comparison with that of control cells (not incubated with NPs). The mean value and standard deviation were obtained from at least six experiments.

Immunofluorescence to detect α-tubulin. Immunofluorescence was carried out in cells grown in coverslips. A-549 cells were fixed in cold methanol (2˚C) for 5 min, washed 3 times during 5 min with PBS, permeabilized 5 min with 0.5% Triton X-100 (v/v), and later incubated with the primary monoclonal mouse anti-α-tubulin antibody (1:100 in PBS/BSA, Sigma) during 1 h at 37˚C in a humidified camera. After washing with PBS three times for 5 min, cells were incubated with the secondary goat anti-mouse antibody fluorescein isothiocyanate (FITC from Sigma) at a dilution 1:100 for 1 h at 37˚C. Finally, cells were washed 3 times for 5 min with PBS, and counterstained with the fluorochrome for

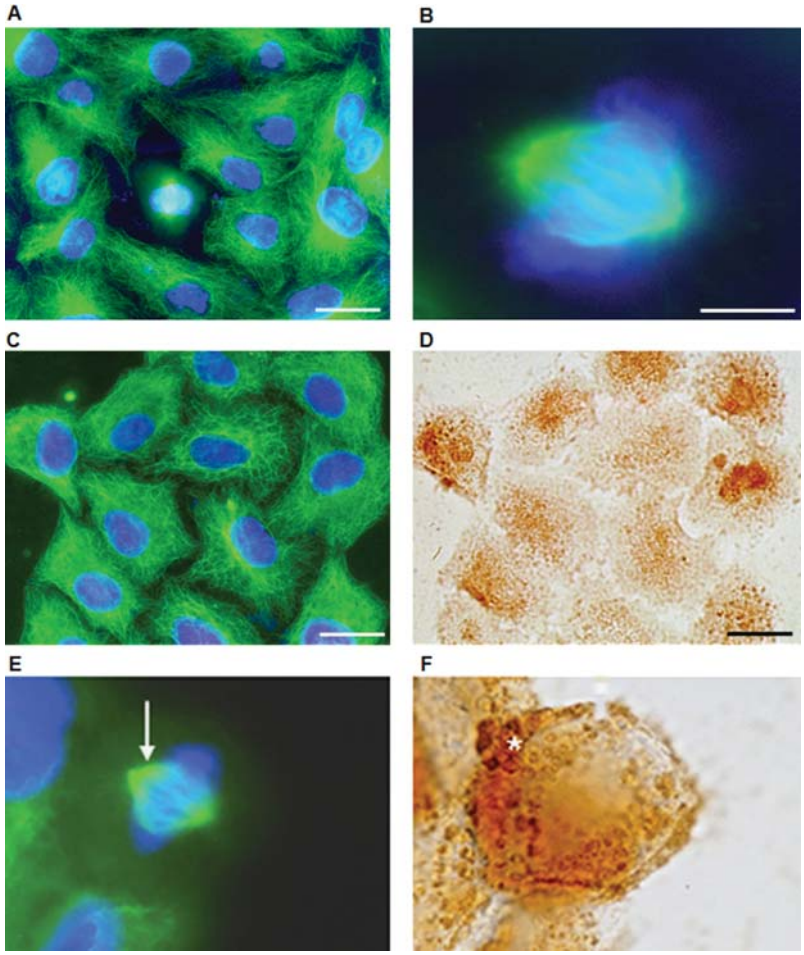

Figure 4. Cells incubated with AD (0.5 mg Fe/ml, 24 h) and processed for immunofluorescence to α-tubulin. Control cells under fluorescence microscopy, (A) interphasic cells, (B) metaphase cells. (C-F) Cells incubated with AD 0.5 mg Fe/ml during 24 h and processed immediately after treatment. (E) Cells observed under fluorescence microscopy. (D) The same field under bright light microscopy. (E) Metaphasic cell (arrow) under fluorescence microscopy. (F) The same mitotic cell showing the NPs in cytoplasm (asterisk) under bright light microscopy. Scale bar 20 μm.

DNA Hoechst-33258 (H-33258, Sigma) at a concentration of 0.05 mg/ml in distilled water, washed with distilled water and mounted in ProLong Gold antifade reagent (Molecular Probes). The fluorescence of FITC (green) and H-33258 (blue) was observed with a fluorescence microscope, using the appropriate excitation filters. The mitotic index (MI) was evaluated in immunofluorescence-processed samples. Four thousand cells were counted for each experimental point of at least three different experiments.

Macropinocytosis inhibition. Serum-deprived A-549 cells were pre-treated with or without 5 μg/ml cytochalasin D (CD, Sigma) for 1 h, followed by co-incubation with NPs (0.1 mg Fe/ml) for 24 h. Cells were washed with PBS 3 times and then observed *in vivo* using bright light microscopy, or stained with tetramethylrhodamine isothiocyanate (TRITC)-labelled phalloidin (TRITC-phalloidin, Sigma) and counter-stained with H-33258.

TRIC-phalloidin stain. For F-actin visualization, cells grown on coverslips were fixed in paraformaldehyde (3%) for 10 min, washed in PBS for 15 min and permeabilized with 0.5% (v/v) Triton X-100 in PBS for 20 min at room temperature. Cells were incubated with TRITC-phalloidin, for 30 min at 37˚C, washed in PBS and counterstained with the fluorochrome for DNA, H-33258 (0.05 mg/ml in distilled water), washed with distilled water and mounted in ProLong Gold. Samples were observed with fluorescence microscopy, using the corresponding excitation filters (545 nm for TRITC-phalloidin and 320 nm for H-33258).

Inhibition of clathrin-dependent endocytosis. A-549 cells were preincubated in serum-free DMEM containing Dynasore 80 μM (Dyn, Sigma) 1 h before incubation with NPs. The media were then changed to fresh ones containing the inhibitors plus AD (0.1 mg Fe/ml) and further incubated for 24 h. After exposure to NPs and inhibitor, cells were washed 3 times with PBS and then observed *in vivo* or processed with toluidine blue for staining.

Microscopy. Microscopic observations and photographs were performed with an Olympus BX61 epifluorescence microscope equipped with ultraviolet (365 nm), blue (420 nm) and green (545 nm) filter sets for fluorescence microscopy and an Olympus DP50 digital camera Micromax; Princeton Instruments.

Results

Nanoparticles. An average particle size of 6 nm was obtained by the coprecipitation of iron salts in the presence of the polymer (sample AD). The particle composition was magnetite. No traces of other iron oxide phases were found by X-ray diffraction. The carbohydrate molecules stabilized the particles in aqueous suspension under physiological conditions (pH and salinity), being the surface potential +26 mV at pH 7.0. Samples were subjected to centrifugation and filtration processes to reduce the hydrodynamic size down to 150 nm with a polydispersity degree of 0.2.

Internalization. The cationic AD applied to A-549 cells was detected inside cells under all experimental conditions. Using a concentration of 0.5 mg Fe/ml, the accumulation of NPs was evident. The evolution of the AD NP-cell interaction was as follows. First (6 h incubation time), NPs formed aggregates outside the cell membrane (Fig. 1B), and 24 h later they were homogeneously distributed into the cell cytoplasm of cells, forming aggregates of variable size (Fig. 1C). These aggregates cannot be detected in control cells (Fig. 1A). Cells retained AD for several hours after the incubation with NPs as is seen in Fig. 1D, showing cells incubated with AD (0.5 mg Fe/ml) for 24 h and observed 48 h after incubation.

In treated cells stained by the toluidine blue method, and incubated with AD (0.5 mgFe/ml), NPs were observed inside cells, with an identical distribution pattern to those observed in living cells (Fig. 2C and D). The cell morphology was similar to control cells (Fig. 2A and B).

Surviving fraction. Fig. 3 shows the surviving fraction of A-549 cells incubated for 24 h at different concentrations of NPs and evaluated by the MTT assay 24 h after treatment. Treated cells showed a survival fraction similar to controls under all experimental conditions.

Microtubules. Possible alterations induced by the nanoparticles in the cytoskeletal components were also evaluated. A-549 cells treated with AD (0.5 mg Fe/ml, 24 h) showed interphasic microtubules (Fig. 4C and D) mitotic spindles and chromosomes (Fig. 4E and F) with a distribution similar to the control cells (Fig. 4A and B). The mitotic index in treated cells was also identical to control cells (4.8±0.2%).

Macropinocytosis inhibition. Macropinocytosis was inhibited by treatment with CD, that inhibits actin filaments polymerization, and transiently alters cell morphology (Fig. 5). Fig. 5A shows the normal distribution of actin filaments in non-treated cells. Samples incubated only with NPs show no significant alteration in actin filaments that remain idetical to control cells. Cells treated with NPs in the presence of CD showed disorganized actin filaments (Fig. 6B) that are identical to those of cells treated only with CD. After 24 h from treatment, cells treated with CD (either alone or in presence of AD) show an actin distribution similar to that of non-treated cells (Fig. 5C).

NP penetration in cells was analyzed by TB staining (Fig. 6). In Fig. 6A, cells incubated with AD (0.1 mg Fe/ml), showing NPs in cytoplasm can be observed. However, when cells were incubated with NP-CD, in most cases AD remained attached to cell membranes, and their incorporation to cytoplasm was strongly inhibited (Fig. 6B).

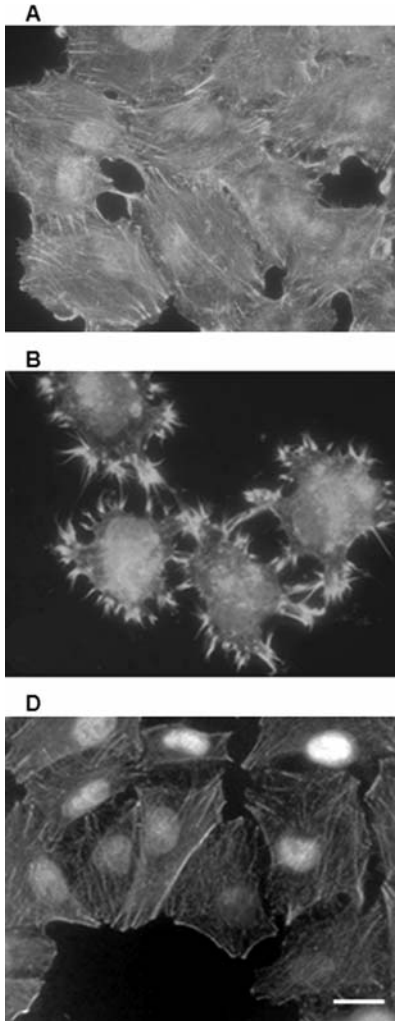

Figure 5. Cells A-549 stained with TRITC-phalloidin and counterstained with H-33258. (A) Control cells, (B) cells incubated with AD (0.1 mg Fe/ml, 24 h) and then processed immediately. (C) Cells co-incubated with AD and CD and processed 24 after treatment. Scale bar 20 μm.

Inhibition of clathrin-dependent endocytosis. Fig. 7 illustrates the results obtained after treatment with inhibitor Dynasore of clathrin mediated endocytosis. As can be seen, the treatment with Dynasore, in absence of AD (Fig. 7B), did not affect the morphology of cells, compared to controls (Fig. 7A). The co-incubation of cells A-549 with Dynasore and AD (0.1 mg Fe/ml) showed a similar amount of accumulation and distribution (Fig. 7C) as cells incubated only with AD (Fig. 7D). This study has proved that Dynasore, used under similar experimental conditions, clearly decreases the penetration of liposomes of dipalmitoyl phosphatidyl choline (DPPC) in A-549 cells (13).

Discussion

Magnetic iron oxide nanoparticles can be coated with a variety of polymers, using different techniques (1,2). In this study, the synthesis was carried out in the presence of AD, whose role is to limit particle growth during the synthesis and provide

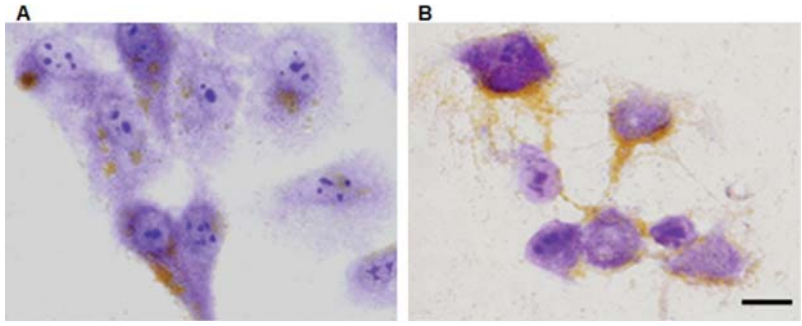

Figure 6. A-549 cells incubated with AD (0.1 mg Fe/ml, 24 h) and processes by TB method immediately after treatments. (A) Cells incubated with AD alone. (B) Cells co-incubated with AD and CD. Scale bar 20 μm.

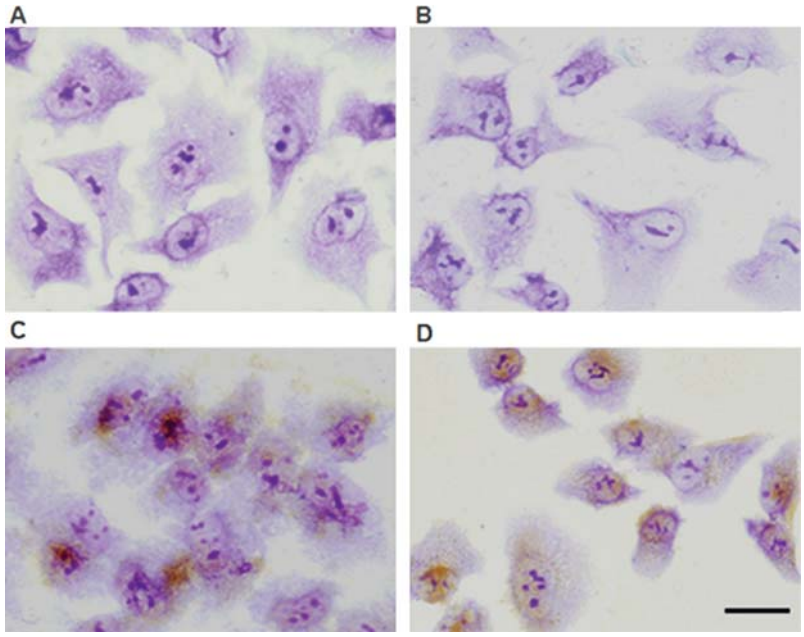

Figure 7. Dynasore effect in A-549 cells, fixed and stained by the TB method immediately after treatments. (A) Control cells; (B) cells incubated with Dyn (25 h); (C) cells incubated with AD (0.1 mg Fe/ml, 24 h); (D) cells preincubated with Dyn for 1 h and co-incubated with AD plus Dyn for 24 h. Scale bar 20 μm.

steric repulsion and positive particle surface charge to stabilise particles in water. Particle size for sample AD was limited to 6 nm (0.2% standard deviation), and the hydrodynamic size, which provides an estimate of the particle aggregate size in suspensions, was reduced by filtration to 150 nm. It is well known that particle and aggregate size, and surface charge, are important factors that determine biocompatibility, distribution in living systems and the specific mechanism of cell internalization of nanoparicles (14).

When NPs are used for therapeutic purposes, size and cover should be optimized to enable their internalization in target cells. They also need to escape the reticulum endothelial system that eliminates NPs from the bloodstream, decreasing or preventing their access to cellular targets (15,14).

There are numerous studies on determining the toxicity of different types of NPs, and it is accepted that NPs covered with positive charge penetrate inside cells more efficiently, reducing toxicity (16,17). Previous results on HeLa cells showed that NPs functionalized with differently charged carbohydrates had different effects on internalization and cell survival (11). Neutral and negative iron oxide nanoparticles were internalized in low quantities or not internalized at all in cells. Furthermore, negative NPs coated with heparin affect cell survival and cycle. However, positive NPs coated with AD were rapidly internalized in cells, and lack of toxicity was observed (11). Similar results were obtained for amino polyvinyl alcohol coated nanoparticles that showed a much higher uptake by cerebral cells, absence of cytotoxicity and *in vivo* biocompatibility (18).

In this study we evaluated biocompatibility of positively charged NPs in A-549 cells, taking into account the influence of cell type. The behaviour of AD in A-549 cells corroborated an easy penetration of these NPs into cells under our experimental conditions, as well as an absence of effects on cell survival. As shown in several figures of this work, morphology of cells incubated with AD did not differ from that of control cells. Elements of cytoskeleton remained organized, even though their distribution was slightly distorted when the amount of internalized NPs was very high. It is also important to note that cells incubated with AD present an

equivalent mitotic index to that of control cells, and mitotic spindles with normal morphology. These results confirm that AD nanoparticles have a significant potential for use in several fields of biomedicine.

On the other hand, the NPs internalization may occur through various endocytic processes that have not been always well identified. The precise knowledge of the endocytosis mechanism is important for the biomedical application of NPs (and any other macromolecule) for therapeutic purposes. The endocytic pathway determines intracellular localization of macromolecules as well as cell-macromolecule interaction (3,4). In this sense, depending on future applications, the mechanism of endocytosis can determine the effectiveness of the treatment. When NPs with appropriate size and cover penetrate cells by clathrin-mediated endocytosis, they accumulate mostly in the lysosomal compartment. If magnetic NPs are used for diagnosis or hyperthermia therapy, their accumulation in lysosomes may not be relevant, but if they are used as carriers of other therapeutic drugs, lysosomal destination is not the most convenient vesicle, because the active substance can be degraded.

A morphological characterization of the possible AD endocytic mechanisms in A-549 cells has been performed. CD is a well known inhibitor of macropinocytosis because it blocks polymerization of actin filaments, which is necessary for this process to occur (19). CD, used in our experimental conditions, affects (immediately after incubation) cell morphology, and also alters the actin cytoskeleton and prevents the incorporation of AD into cells. Under these conditions, NPs remain adhered to the plasma membrane and are detected in very small quantities in cytoplasm. Although cells processed immediately after incubation with CD appear morphologically altered, this cellular change is reversible, and 24 h later cell morphology is normal. These results confirm that the majority of cells remain alive after incubation with CD. Some authors have described that inhibition of dynamic polymerization of actin may also affect clathrin mediated endocytosis (20), but this inhibition depends on several factors, namely treatment dose and cell type (21). In this sense, it is not possible to exclude that CD, under our experimental conditions, also inhibits the receptor mediated endocytosis process.

Dynasore is a specific inhibitor of dynamin activation that perturbs the linkage Dyn is an inhibitor of the dynamin activation that perturbs the linkage of dynamin to clathrin, which is a key process in clathrin-mediated endocytosis (22). Treatment of A-549 cells with this inhibitor does not affect penetration of NPS in cells, enabling the observation of identical accumulation of NPs and cell morphology in cells incubated with AD alone and in cells incubated with AD-Dyn. In our previous studies we were able to assess that experimental conditions used in these experiments with Dyn inhibited penetration of DPPC liposomes in A-549 cells, but, on the other hand, CD does not affect penetration of liposome containing ZnPc (13). This ensures that experimental conditions used for Dyn in this study produce inhibition of the endocytic process. Thus, although clathrin-mediated endocytosis was inhibited, AD-NPs penetrated cells similarly as in cells not treated with the inhibitor. This indicates that the endocytic process is not preferentially used by AD to penetrate into cells.

In conclusion, cationic magnetic nanoparticles penetrate easily into A-549 cells, remaining in cells for long periods of time. NP internalization did not alter either cell viability or morphologic parameters, under any of our experimental conditions. Co-incubation of cells with nanoparticles and specific inhibitors of endocytic process shows that nanoparticles are internalized into cells mainly by a macropinocytosis process. Both absence of toxicity and mechanism of internalization suggest that cationic particles are suitable candidates for diagnosis, hyperthermia therapy and as a carrier of different therapeutic drugs.

Acknowledgements

This work was supported by a grant from Comunidad Autónoma de Madrid (S-0505 MAT-0194) and the MICIIN (Consolider on Molecular Nanoscience).

References

1. Gupta AK and Gupta M: Cytotoxicity suppression and cellular uptake enhancement of surface modified magnetic nanoparticles. Biomaterials 26: 1565-1573, 2005.
2. Lin MM, Kim do K, El Haj AJ and Dobson J: Development of superparamagnetic iron oxide nanoparticles (SPIONS) for translation to clinical applications. IEEE Trans Nanobioscience 7: 298-305, 2008.
3. Bareford LM and Swaan P: Endocytic mechanisms for targeted drug delivery. Adv Drug Deliv Rev 59: 748-758, 2007.
4. Greco F and Vicent MJ: Polymer-drug conjugates: current status and future trends. Front Biosci 1: 2744-2756, 2008.
5. Sun C, Lee JS and Zhang M: Magnetic nanoparticles in MR imaging and drug delivery. Adv Drug Deliv Rev 60: 1252-1265, 2008.
6. Hosseinkhani H and Tabata Y: Self assembly of DNA nanoparticles with polycations for the delivery of genetic materials into cells. J Nanosci Nanotechnol 23: 20-28, 2006.
7. Gupta AK, Naregalkar RR, Vaidya VD and Gupta M: Recent advances on surface engineering of magnetic iron oxide nanoparticles and their biomedical applications. Nanomed 2: 23-39, 2007.
8. Petri-Fink A, Chastellain M, Juillerat-Jeanneret L, Ferrari A and Hofmann H: Development of functionalized superparamagnetic iron oxide nanoparticles for interaction with human cancer cells. Biomaterials 26: 2685-2694, 2005.
9. Ma YJ and Gu HC: Study on the endocytosis and the internalization mechanism of aminosilane-coated Fe_3O_4 nanoparticles in vitro. J Mater Sci Mater Med 18: 2145-2149, 2007.
10. Wilhelm C and Gazeau F: Universal cell labelling with anionic magnetic nanoparticles. Biomaterials 29: 3161-3174, 2008.
11. Villanueva A, Cañete M, Roca AG, Calero M, Veintemillas-Verdaguer S, Serna CJ, Morales Mdel P and Miranda R: The influence of surface functionalization on the enhanced internalization of magnetic nanoparticles in cancer cells. Nanotechnology 20: 115103, 2009.
12. Xu XQ, Shen H, Xu JR, Xu J, Li XJ and Xiong XM: Core-shell structure and magnetic properties of magnetite magnetic fluids stabilized with dextra. Appl Surface Sci 252: 494-500, 2005.
13. Soriano J, Stockert JC, Villanueva A and Cañete M: Cell uptake of Zn(II)-phthalocyanine-containing liposomes by clathrin-mediated endocytosis. Histochem Cell Biol 133: 499-454, 2010.
14. Xu F, Yuan Y, Shan X, Liu C, Tao X, Sheng Y and Zhou H: Long-circulation of hemoglobin-loaded polymeric nanoparticles as oxygen carriers with modulated surface charges. Int J Pharm 377: 199-206, 2009.
15. Chouly C, Pouliquen D, Lucet I, Jeune JJ and Jallet P: Development of superparamagnetic nanoparticles for MRI: effect of particle size, charge and surface nature on biodistribution. Microencapsulation 13: 245-255, 1996.
16. Bennett KM, Zhou H, Sumner JP, Dodd SJ, Bouraoud N, Doi K, Star RA and Koretsky AP: MRI of the basement membrane using charged nanoparticles as contrast agents. Nanomed 4: 9-10, 2009.

17. Shieh DB, Cheng FY, Su CH, Yeh CS, Wu MT, Wu YN, Tsai CY, Wu CL, Chen DH and Chou CH: Aqueous dispersions of magnetite nanoparticles with NH^{3+} surfaces for magnetic manipulations of biomolecules and MRI contrast agents. Biomaterials 26: 7183-7191, 2005.
18. Cengelli F, Maysinger D, Tschudi-Monnet F, Montet X, Corot C, Petri-Fink A, Hofmann H and Juillerat-Jeanneret L: Interaction of functionalized superparamagnetic iron oxide nanoparticles with brain structures. J Pharmacol Exp Ther 318: 108-116, 2006.
19. Peterson JR and Mitchison TJ: Small molecules, big impact: a history of chemical inhibitors and the cytoskeleton. Chem Biol 9: 1275-1285, 2002.
20. Kaksonen M, Toret CP and Drubin DG: Harnessing actin dynamics for clathrin-mediated endocytosis. Nat Rev Mol Cell Biol 7: 404-414, 2006.
21. Fujimoto LM, Roth R, Heuser JE and Schmida SL: Actin Assembly plays a variable, but not obligatory role in receptor-mediated endocytosis in mammalian cells. Traffic 1: 161-171, 2000.
22. Lu W, Ma H, Sheng ZH and Mochida S: Dynamin and activity regulate synaptic vesicle recycling in sympathetic neurons. J Biol Chem 16: 1930-19377, 2009.